Slip trace-induced terrace erosion

Benjamin Douat[1], Jérôme Colin[1,2], Roberto Bergamaschini[2], Francesco Montalenti[2], Michel Drouet[1], Joël Bonneville[1], Christophe Coupeau[1]

[1] *Institut P', UPR 3346 CNRS/Universtté de Potiers/ENSMA, SP2MI-Téléport 2, F86962 Futuroscope-Chasseneuil cedex, France*

[2] *Department of Materials Science, University of Milano-Bicocca, Via R. Cozzi 55, I-20125 Milan, Italy*

Abstract

We have investigated the interaction between slip traces and vicinal steps on the Nb(111) surface under increasing external strain. By exploiting an extended scanning tunneling microscopy analysis, we here show that emerging dislocations at the free-surface can induce the full disappearance of atomic terraces. To shed light on the observed behavior, we have modeled the elastic interaction between a screw dislocation and a vicinal step in the actual experimental configuration. After computing the adatom chemical potential, we show that strain-mediated diffusion on surface causes step erosion, possibly leading to vanishing of full terraces.

Keywords:
STM observations, plasticity, dislocations, surface diffusion, terrace evolution

1. Introduction

The study of the surface evolution of nanostructured materials is a topic of extensive researches in the fields of surface physics, materials science and metallurgy because of the numerous applications of such materials in various engineering fields such as nanoelectronics or nanophotonics. For instance, it has been observed that faceted macrosteps can deteriorate the quality of grown crystals [1] and, in the particular case of 4H-SiC, it has been reported that faceted steps perturb the performance of electric devices. It is also well-known that vicinal surfaces can be used as templates for growing layers with controlled orientation and crystallinity. Recently, the case of Ag growth on

a Ni(11, 9, 9) substrate has been studied and a Stranski-Krastanov growth mode has been observed to take place leading to the formation of a wetting layer of two monolayers with well-crystallized islands [2]. Likewise, the specific orientation of the substrate has been found to produce Ag thin films with Ag(7, 9, 9) orientation such that neither twin nor stacking fault has been reported. From a numerical point of view, the formation and dynamical evolution of these faceted steps have been meanwhile investigated by means of Monte-Carlo simulations and the classical 2D heterogeneous multinucleation theory has been proved to be valid [3].

Residual stress lying in polycrystalline thin films has also been identified as a determinant parameter controlling the thermomechanical fatigue of the devices in which the polycrystalline thin films are introduced [4]. In particular, the insertion of adatoms in grain boundary has been found to be responsible for compression stress leading to mechanical failures. It has been then demonstrated that the compressive stresses are located at the edges of gaps where the grain boundaries reach the surface [5]. Likewise, stress usually associated with plasticity phenomena in the bulk of crystalline materials can modify their surface structure. It has been for instance found that stresses can influence the reconstruction of Si(001) [6, 7] or Si(111) surfaces [8], the chevron-like Au(111) reconstruction as well [9, 10]. In case of Au films grown on W(110) substrate, the interface stress and edge dislocation loops have also been found to modify the reconstruction pattern [11].

Another example is concerned with gliding dislocations generated in the bulk that can lead to the formation of slip traces at the solid surfaces. These slip traces can then interact with the vicinal steps [12, 13]. Recently, it has been found that slip traces and surface diffusion deeply modify the organization (morphology and height) of vicinal steps at the surface of Au(111) strained single crystal samples [14]. In particular, the regions where the vicinal steps and slip traces intercept have been found to undergo mass diffusion.

In this work, the effects of crystalline plasticity on the evolution of atomic terraces of strained niobium single crystals have been investigated by both experiments and modeling. The terrace erosion due to slip traces induced by moving screw dislocations located below the surface has been then characterized. The effect of atomic diffusion onto the terrace evolution has been finally analyzed by means of a simple attachment-detachment kinetic model based on the calculation of the chemical potential.

2. experimental observations

Nb single crystals of nominal section 2×2 mm^2 and 6 mm length were prepared by Surface Preparation Laboratory [15]. The Nb($1\bar{1}1$) surface was oriented with an accuracy better than 0.1°. After a chemical/mechanical polishing, the Nb($1\bar{1}1$) surface was then prepared under UHV environment ($< 10^{-10}$ mbar) by repeated cycles of Ar ion bombardments (0.9 kV for 10 min) and annealing at 1000°C for 2 h. After a few cycles, the surface exhibits atomically flat {111} terraces separated by vicinal steps (Fig. 1) on which the energetically favorable (2×2) reconstruction [16] is clearly distinguishable (see insert for a zoom of the atomic structure). The samples were then mechanically strained in UHV conditions at 200 K using a home-made experimental device allowing to characterize by scanning tunneling microscopy (STM) the *in situ* evolution of surfaces under increasing strain (see [17] for more details). The uniaxial compression stress was applied along the [$\bar{1}12$] direction. From crystallographic considerations, the [111]($\bar{1}01$) and [$11\bar{1}$](011) slip systems are expected to be activated in Nb bcc single crystals [18, 19], resulting in slip traces lying on the Nb($1\bar{1}1$) surface along the [121] and [$\bar{2}\bar{1}1$] directions respectively, at $\pm 60°$ from the compression axis. The height h of a single slip trace (*i.e.* a slip trace resulting from the emergence of only one perfect moving dislocation) is equal to the Burgers vector $\mathbf{b}$ component perpendicular to the free surface. Theoretically, $h = \mathbf{n}.\mathbf{b} = \frac{\sqrt{3}}{2}a = 0.95$ nm, with $\mathbf{n}$ the normal to the free surface and $a = 0.33$ nm the niobium lattice parameter. Finally, it must be noted that the height of vicinal steps is necessarily proportional to h, as experimentally checked in Fig. 1.

A STM investigation of the Nb($1\bar{1}1$) surface after a plastic strain ϵ_p of 1.51% is presented in Fig. 2a. As expected, slip traces (labeled from T_1 to T_4) are lying along the [121] direction at $-60°$ from the compression axis. The height of each slip trace is experimentally found to be 97 pm, close to the theoretical 95 pm value. It confirms that they are related to a single [111] screw dislocation in the bulk. The dislocation cores are located at the free surface at the end of the slip traces (see the white stars). Two vicinal steps are also evidenced in Fig. 2, labeled V_1 and V_2. A characteristic STM profile crossing the vicinal steps is presented in Fig. 2c (see the black dash line for exact position in Fig. 2a). Their heights are 0.3 nm and 1.5 nm for V_1 and V_2, respectively. It is observed that the four dislocation cores are located very close to V_1. The same area has been characterized approximately 50

min after, following a slight plastic strain increment of $\Delta\epsilon_p = 0.02\%$. It is observed in Fig. 2b that the terrace between V_1 and V_2 has disappeared. For the sake of clarity, the previous position of the terrace has been reported as white hatched area in Fig. 2b. The two STM profiles have been superimposed in Fig. 2c as an experimental proof of such an erosion of the atomic terrace. A rough estimate of the involved surface leads to 400 nm^2. It strongly suggests a significant atomic diffusion process induced by the dislocation estimated to be of the order of 4800 atoms. It can also be observed that three of the four dislocations (see the slip traces T_1, T_3 and T_4) slightly propagated after the increase of plastic strain, of only a few nanometers. It is believed here that the moving dislocations have enhanced the erosion of the atomic terrace previously mentioned. Finally, it is underlined that several experimental STM sequences have been performed (but not shown) to confirm that the observed phenomena described in this section are fully identified and properly characterized.

3. Modeling and discussion

In agreement with the previous experimental observations, the following configuration described in Fig. 3 has been considered. A slip trace of height $h = 0.1$ nm (labeled T) resulting from the emergence of a gliding dislocation is lying in the neighborhood of two vicinal steps V_1 and V_2 of infinite length and height h_1 and h_2, respectively, with $h_1 = 0.3$ nm and $h_2 = 1.5$ nm. The distance between V_1 and the emerging point of the dislocation (*i.e.* position of the dislocation core at the free surface) is labeled d, the one between V_2 and the emerging point, D, the angle between the normal of the two terraces and the trace direction being labeled θ. For the sake of simplicity, only one screw dislocation perpendicular to the free-surface has been taken into account, the Burgers vector being thus $\mathbf{b} = (0, 0, b)$. Since h_2 is of the order of several atomic planes, V_2 is assumed to be motionless in the following. For the surface under external loading compressive stress $\sigma^0_{xx} = -\sigma_0$, with σ_0 a positive constant, the elastic interactions between the two vicinal steps and the slip trace have been modeled in the force monopole approximation of the linear isotropic theory of elasticity [20] for a solid of Young modulus E and Poisson ratio ν [21, 22, 23, 24, 25]. The slip trace is also assumed to be motionless in this approach, and one will focus on the equilibrium position of V_1. The stress field of the dislocation of Burgers vector $\mathbf{b}$ located below the surface has already been determined in [26] and its derivation is not explicitly

presented in this work. In a first static approach, the elastic interaction energies between V_1, V_2 and T have been determined in the hypothesis where the strain along the normal direction to the surface is constant, such that the force monopole approximation can be used [21, 22, 23, 24, 25]. In this framework, distributions of force monopoles $\mathbf{f}_{V_1} = h_1\sigma_0\mathbf{i}$ on the V_1 step and $\mathbf{f}_T = h\sigma_0 \sin^2\theta(\sin\theta\mathbf{i}+\cos\theta\mathbf{j})$ for the slip trace have been introduced to model the elastic relaxation due to the stepped surface. A distribution $\mathbf{f}_{V_2} = h_2\sigma_0\mathbf{i}$ on the V_2 step is equivalently introduced. The elastic interaction potential Φ_{T-V_1} between V_1 and T depending on d variable has been then expressed as [21]:

$$\begin{aligned}\Phi_{T-V_1} &= -\frac{1}{2}\int_{-L}^{L}\int_{-L'}^{L'}\Big[\frac{1-\nu^2}{\pi E}\frac{\mathbf{f}_T\mathbf{f}_{V_1}}{|\mathbf{r}'-\mathbf{r}|} \\ &+ \frac{\nu(1+\nu)}{\pi E}\frac{(\mathbf{f}_T(\mathbf{r}'-\mathbf{r}))(\mathbf{f}_{V_1}(\mathbf{r}'-\mathbf{r}))}{|\mathbf{r}'-\mathbf{r}|^3}\Big]d\mathbf{r}'d\mathbf{r}, \end{aligned} \tag{1}$$

with $2L$ and $2L'$ the considered length of the step and trace, respectively. Integrating Eq. (1) and taking $L, L' \to \infty$ allows for calculating the elastic interaction potential Φ_{T-V_1}. The force exerted by T onto V_1 (per unit length) is thus derived as:

$$\mathbf{f}_{T/V_1} = -\frac{d\Phi_{V_1T}}{dx_d}\mathbf{i} = \frac{(1-\nu^2)\sigma_0^2 h h_1}{\pi E}\frac{\sin^4\theta}{d}\mathbf{i}. \tag{2}$$

It can be observed from Eq. (2) that as the maximum interaction force between T and V_1 step is obtained for two parallel structures ($\theta = \pi/2$), the force $\mathbf{f}_{T/V_1}$ cancelling for perpendicular step, *i.e.* for $\theta = 0$. Likewise, the Marchenko force exerted by V_2 on V_1 is given by [21]:

$$\mathbf{f}_{V_2/V_1} = -\frac{(1-\nu^2)\sigma_0^2 h_1 h_2}{2\pi E}\frac{1}{D-d}\mathbf{i}. \tag{3}$$

The energy terms due to the elastic interaction between the dislocation and V_1, V_2 and T are also considered. Due to the screw character of the dislocation and to the symmetry of the problem, these contributions have been found to cancel. Once the elastic energy is known, a constant average force exerted onto the whole V_1 step moving along (Ox) axis has been defined as: $\mathbf{f} = \mathbf{f}_{T/V_1} + \mathbf{f}_{V_2/V_1} = f\mathbf{i}$, where it is assumed in a first approximation that the straight shape of the step is preserved. In Fig. 4, the reduced total force

f/f_0 has been plotted versus d/D for different values of the angle θ, with $f_0 = (1-\nu^2)\sigma_0^2 h_1 h_2/[2\pi E(D-d)]$. Writing the equilibrium condition $\mathbf{f} = 0$ allows for defining an unstable position d_c for the V_1 step given by:

$$d_c = D\Big(1 + \frac{h_2}{2h\sin^4\theta}\Big)^{-1}. \tag{4}$$

For a height ratio $h_2/h \sim 15$, one gets $d_c < 0.133D$ (for $\theta < \pi/2$) such that it can be concluded at this point that due to elasticity effect, the emerging point should be almost at the contact with the V_1 step, as observed in our experiments. On the reverse, a single vicinal step V_2 for which h_2=h leads to an equilibrium distance of $2/3D$ for $\theta = \pi/2$, so that V_1 is no more in the neighborhood of T.

In order now to investigate the kinetic evolution of V_1 under controlled temperature $T = 200$ K, the effects of adatom diffusion on the terrace morphological change and erosion have been analyzed by a simple model. Assuming that the adatoms migrate in the field of the chemical potential, the first step has been to calculate the elasticity contribution μ to the chemical potential in the case of straight steps. Additional contributions to the chemical potential, such as the step line energy, are expected to play a minor role and are not included in the following. Introducing ϕ the total elastic potential taking into account ϕ_{V_1/V_2} the interaction energies between the two steps V_1 and V_2, ϕ_{T/V_1} and ϕ_{T/V_2} the interaction energies between the trace T and the two steps V_1 and V_2, $\phi_{\star/V_1}$, $\phi_{\star/V_2}$ and $\phi_{\star/T}$ the interaction energies between the dislocation beneath the surface ($\star$) and the two steps V_1 and V_2 and the slip trace T, respectively, the chemical potential of adatoms μ is defined as:

$$\begin{aligned}
\mu &= \frac{\delta\phi}{\delta N} \\
&= v_a \frac{\delta}{\delta v}(\phi_{V_1/V_2} + \phi_{T/V_1} + \phi_{T/V_2} + \phi_{\star/V_1} \\
&+ \phi_{\star/V_2} + \phi_{\star/T}) \\
&= v_a \frac{1}{2} tr(\bar{\bar{\sigma}}\bar{\bar{\epsilon}}),
\end{aligned} \tag{5}$$

where N is the number of atoms, v the corresponding volume variable, v_a the atomic volume, $\bar{\bar{\sigma}}$ and $\bar{\bar{\epsilon}}$ the total stress and strain tensors, respectively. The details of the calculations and the resulting cumbersome analytical expression of μ for a straight step are not presented here. Once the elasticity term μ

of the chemical potential is known, the diffusion process can be investigated considering the adatom flux is assumed to be directed onto the surface from the regions of high μ towards the regions of low μ. In Fig. 5, μ has been plotted versus x and y variables, taking the following parameters, $\theta = 60^{\circ}$, $\sigma_0 = 167$ MPa, $h = 0.1$ nm, $h_1 = 0.3$ nm and $h_2 = 1.5$ nm. The Young modulus and Poisson ratio of Nb are taken to be $E = 105$ GPa and $\nu = 0.35$, respectively. It thus appears on Fig. 5a that μ is maximum in the neighborhood of the emerging point of the dislocation and the V_1 step, and decreases from this region to infinity, the adatoms being thus supposed to diffuse far away from this step-dislocation region onto the terraces. This decrease of the chemical potential is particularly marked along the step line as one leaves the region close to the dislocation emerging point.

The kinetic evolution of the V_1 step, characterized by the profile function depending on both variables x and y was then modeled as resulting from the attachment-detachment dynamics of adatoms at the V_1 step edge, assuming fast-diffusion of the released adatoms on top of the terraces. The motion of the step can be traced as the function $y(x,t)$, according to the evolution equation [27]:

$$\frac{dy}{dt} = -k[\mu(x,y) - \mu_0], \tag{6}$$

where k is a non-dimensional coefficient and t is the nondimensional time. The long-range transport has been considered such that the material detachment or attachment is assumed to take place for $\mu > \mu_0$ or $\mu < \mu_0$, respectively. μ_0 is the reference chemical potential of the step far from the dislocation, as given by $\lim_{y\to\infty} \mu(x,y) \sim 0.064$ meV. Moreover, line diffusion (here neglected) could also positively contribute to the shape evolution of the step. A cut-off of the order of 0.3 nm corresponding to the lattice parameter of Nb($1\bar{1}1$) surface has also been used to avoid any elasticity divergence at the V_1 elastic singularity. Although the expression of the chemical potential of the initial straight step is not upgraded as the step deforms, the numerical integration of the eq. 6 is performed by updating at each time increment the value of $\mu = \mu(x(t), y)$ at each point of the deformed profile of the step. This approximation is assumed to give reasonably accurate values of μ while considering small amplitudes of the shape modification, up to ~ 2 nm, as reported in panels (b) and (c) of Fig. 5 for evolution times up to 1 (in arbitrary units, a.u.). This approximation does not allow to investigate the long-term

behavior. Still, the initial evolution strongly suggests a possible scenario explaining the experimental data. Indeed, it is clearly observed in Fig. 5 that due to the elasticity effect, the step undergoes a meander evolution leading to a local erosion of the terrace, in the vicinity of the dislocation slip trace. Later stages (t=10 and 20 a.u.) are also reported in panel (b) to qualitatively sketch the possible continuation of the step retraction toward V_2. In order to explain the full disappearance of the V_1 step, the following scenario can now be drawn. Assuming each dislocation generating a slip trace that moved close to the V_1 step can lead to the meander evolution here observed, a full strip of terrace can be thus retrieved when the different meanders overlap for a given periodic distribution of slip traces. It is suspected that the phenomenon is enhanced when dislocations are moving due to an increase of the applied stress that is carried out in our experiments.

4. Conclusion

The decisive role of slip traces generated by moving screw dislocations has been experimentally evidenced on the terrace disappearance observed on the surface of niobium single crystals under controlled stress and temperature. Taking into account the elastic interactions between vicinal steps and slip traces, a simple model suggests that the formation of a meander due to adatom diffusion in the field of the chemical potential may explain the terrace erosion.

5. Acknowledgments

This work was partially funded by the French Government program Investissements d'Avenir (LABEX INTERACTIFS, reference ANR-11-LABX-0017-01) and was financially supported by the Region Poitou-Charentes.

6. References

[1] T. Mitani, N. Komatsu, T. Takahashi, T. Kato, S. Harada, T. Ujihara, Y. Matsumoto, K. Kurashige, H. Okumura, Effect of aluminum addition on the surface step morphology of 4HSiC grown from SiCrC solution, J. Cryst. Growth **423** (2015) 45-49.

[2] A. Bellec, Y. Garreau, J. Creuze, A. Vlad, F. Picca, M. Sauvage-Simkin, A. Coati, Ag on a Ni vicinal surface: Coupling Stranski-Krastanov and magic heteroepitaxial growth, Phys. Rev. B **96** (2017) 085414.

[3] N. Akutsu, Height of a faceted macrostep for sticky steps in a step-faceting zone, Phys. Rev. Mat. **2** (2018) 023603.

[4] F. C. Campbell , Elements of Metallurgy and Engineering Alloys, edited by ASM International, Materials Park, Chap. 14 (2008).

[5] E. Vasco, C. Polop, Intrinsic Compressive Stress in Polycrystalline Films is Localized at Edges of the Grain Boundaries, Phys. Rev. Lett. **119** (2017) 256102.

[6] F. K. Men, W. E. Packard, M. B.Webb, Si(100) surface under an externally applied stress, Phys. Rev. Lett. **61** (1988) 2469-2471.

[7] D. Fujita, M. Kitahara, K. Onishi, K. Sagisaka, An atomic resolution scanning tunneling microscope that applies external tensile stress and strain in an ultrahigh vacuum, Nanotechnology **19**(2) (2008) 025705.

[8] Y. Wei, L. Li, I.S.T.Tsong, Surface morphology of Si(111) $-$ (7×7) under an external isotropic tensile stress, J. Vac. Sci. Technol. A **13** (1995) 1609.

[9] O. Schaff, A.K. Schmid, N.C. Bartelt, J. de la Figuera, R.Q. Hwang, In-situ STM studies of strain-stabilized thin-film dislocation networks under applied stress, Mat. Science and Eng. A **319** (2001) 914-918.

[10] D. Chauraud, J. Durinck, M. Drouet, L. Vernisse, J. Bonneville, C. Coupeau, Influence of terrace widths on Au(111) reconstruction, Phys. Rev. B **96** (2017) 041405.

[11] T. Giela, K. Freindl, N. Spiridis, J. Korecki, Au(111) films on W(110) studied by STM and LEED - Uniaxial reconstruction, dislocations and Ag nanostructures, Appl. Surf. Sci. **312** (2014) 91-96.

[12] H. Höche, J. P. Toennies, R. Vollmer, Combined electron-microscope surface-decoration and helium-atom-scattering study of the layer-by-layer photon-stimulated desorption from NaCl cleavage faces, Phys. Rev. B **50** (1994) 679-691.

[13] I.O. Akhundov, D.M. Kazantsev, V.L. Alperovich, N.S. Rudaya, E.E. Rodyakina, A.V. Latyshev, Formation and interaction of dislocation-induced and vicinal monatomic steps on a GaAs(001) surface under stress relaxation, Script. Mater. **114** (2016) 125-128.

[14] C. Coupeau, O. Camara, M. Drouet, J. Durinck, J. Bonneville, J. Colin, J. Grilhé, Slip-trace-induced vicinal step destabilization, Phys. Rev. B **93** (2106) 041405(R).

[15] Surface Preparation Laboratory B.V., Penningweg 69 F 1507 DE Zaandam The Netherlands, www.spl.eu

[16] C. Coupeau, J. Durinck, M. Drouet, B. Douat, J. Bonneville, J. Colin, J. Grilh, Atomic reconstruction of niobium (111) surfaces, Surf. Sci. **632** (2015) 60-63.

[17] Y. Nahas, F. Berneau, J. Bonneville, C. Coupeau, M. Drouet, B. Lamongie, M. Marteau, J. Michel, P. Tanguy, C. Tromas, An experimental UHV AFM-STM device for characterizing surface nanostructures under stress/strain at variable temperature, Rev. Sci. Instrum. **84** (2013) 105117.

[18] C. R. Weinberger, B. L. Boyce, C. C. Battaile, Slip planes in bcc transition metals, Inter. Mater. Reviews, **58** (2013) 296-314.

[19] C. Marichal, H. Van Swygenhoven, S. Van Petegem, C. Borca, {111} Slip with {112} slip traces in bcc tungsten, Sci. Rep. **3** (2013) 2547.

[20] L.D. Landau, and E.M. Lifshitz, Theory of Elasticity, Pergamon Press Ltd. **7** (1970) 27-30.

[21] V.I. Marchenko, A.Ya. Parshin, Elastic Properties of the Crystal Surface, JETP **52** (1980) 129-131.

[22] O.L. Alerhand, D. Vanderbilt, R.D. Meade, J.D. Joannopoulos, Spontaneous Formation of Stress Domains on Crystal Surfaces, Phys. Rev. Lett. **61** (1988) 1973-1976.

[23] J. Tersoff, and R.M. Tromp, Shape transition in growth of strained islands: Spontaneous formation of quantum wires, Phys. Rev. Lett. **70** (1993) 2782-2786.

[24] A. Li, F. Liu, M.G. Lagally, Equilibrium Shape of Two-Dimensional Islands under Stress, Phys. Rev. Lett. **85** (2000) 1922-1925.

[25] F. Liu, Handbook of Theoretical and Computational Nanotechnology, eds by M. Rieth, W. Schommers, American Scientific Publishers, City **4** (2006) 577-625.

[26] J. D. Eshelby, and A. N. Stroh, Dislocations in thin plates, The London, Edinburgh and Dublin Philosophical Magazine and Journal of Science **42** (1951) 1401-1405.

[27] R. Bergamaschini, M. Salvalaglio, R. Backofen, A. Voigt, F. Montalenti, Continuum modelling of semiconductor heteroepitaxy: an applied perspective, Adv. Phys. X **1** (2016) 331-367.

Figure 1: Nb(1$\bar{1}$1) surface investigated by STM at room temperature exhibiting flat (1$\bar{1}$1) terraces separated by vicinal steps (white lines). The (2 × 2) atomic reconstruction is highlighted in insert.

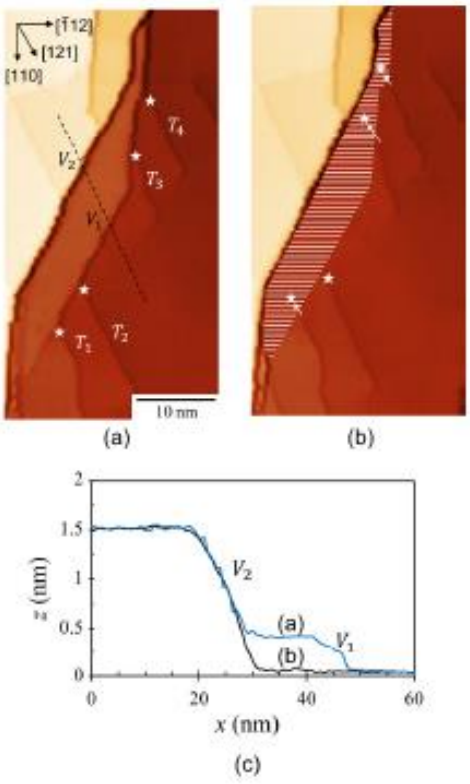

Figure 2: STM investigations of the Nb($1\bar{1}1$) surface at two different plastic strain (a) $\epsilon_p = 1.51\%$ and (b) $\epsilon_p = 1.53\%$. The slip traces (resp. the vicinal steps) are labeled from T_1 to T_4 (resp. V_1 and V_2). The positions of the dislocation cores are symbolized by white stars. The cross sections extracted on the black dashed line in (a) and (b) have been reported in (c).

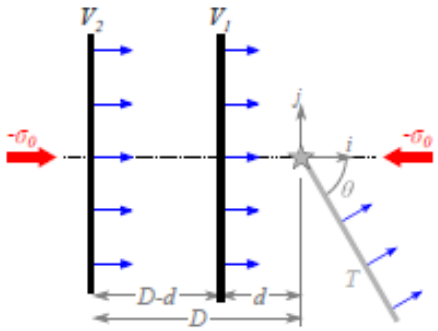

Figure 3: Schematic of two vicinal steps V_1 and V_2 (black lines) and of a slip trace T (grey line) generated by the gliding of a screw dislocation lying below the Nb free-surface. The distances between V_1 (resp. V_2) and the emerging point of the dislocation at the free surface (star symbol) are labeled d (resp. D). Distributions of force monopoles are introduced on the steps and trace to model the elastic relaxation of the solid under the compression stress $-\sigma_0$.

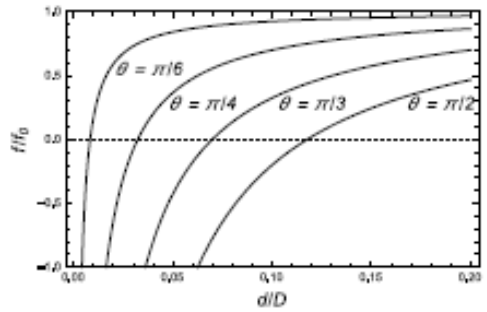

Figure 4: Reduced force f/f_0 versus d/D for different values of the inclination angle θ of the trace with respect to the normal direction of the vicinal steps (for $\sigma_0 = 167$ MPa, $h = 0.1$ nm, $h_1 = 0.3$ nm, $h_2 = 1.5$ nm, $E = 105$ GPa and $\nu = 0.35$)

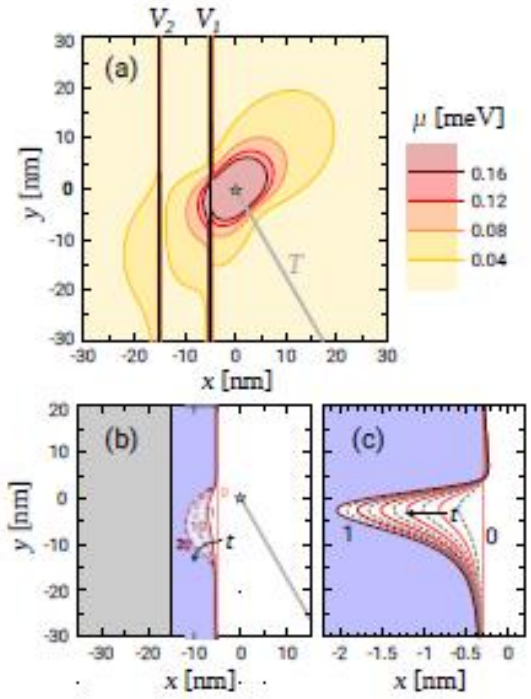

Figure 5: (a) Contourplot of the chemical potential μ versus (x, y) onto the niobium surface, near the steps V_1 and V_2 and the trace T. (b) Time evolution of the vicinal step V_1 versus time. (c) Focus on the early time increments. (For $\theta = 60°$, $\sigma_0 = 167$ MPa, $h = 0.1$ nm, $h_1 = 0.3$ nm, $h_2 = 1.5$ nm, $\mu = 105$ GPa and $\nu = 0.35$).